Title: The inhibitory influence of adipose tissue-derived mesenchymal stem cell environment and Wnt antagonism on breast tumour cell lines

Authors: Malini Visweswaran[1], Frank Arfuso[1], Rodney J. Dilley[2], Philip Newsholme[3], Arun Dharmarajan[1*]

[1]Stem Cell and Cancer Biology Laboratory, School of Biomedical Sciences, Curtin Health Innovation Research Institute, Curtin University, Western Australia, Australia

[2]Ear Sciences Centre, University of Western Australia, Western Australia, Australia

[3]School of Biomedical Sciences, Curtin Health Innovation Research Institute, Curtin University, Western Australia, Australia

Email addresses for authors:

malini.visweswaran@postgrad.curtin.edu.au

frank.arfuso@curtin.edu.au

rodney.dilley@earscience.org.au

Philip.Newsholme@curtin.edu.au

a.dharmarajan@curtin.edu.au

* Corresponding author:

Professor Arun Dharmarajan, Stem Cell and Cancer Biology Laboratory, School of Biomedical Sciences, Curtin Health Innovation Research Institute, Curtin University, Perth WA, Australia. 6102

Email: a.dharmarajan@curtin.edu.au

Tel: +61 8 9266 9867. Fax: +61 8 9266 2342

ABSTRACT

Tumours exhibit a heterogeneous mix of cell types that reciprocally regulate their growth in the tumour stroma, considerably affecting the progression of the disease. Both adipose-derived mesenchymal stem cells and Wnt signalling pathway are vital in driving breast tumour growth. Hence, we examined the effect of secreted factors released by adipose-derived mesenchymal stem cells, and further explored the anti-tumour property of the Wnt antagonist secreted frizzled-related protein-4 on MCF-7 and MDA-MB-231 breast tumour cells.

We observed that conditioned medium and extracellular matrix derived from adipose-derived mesenchymal stem cells inhibited tumour viability. The inhibitory effect of the conditioned medium was retained within its low molecular weight and non-protein component. The conditioned medium also induced apoptosis accompanied by a decrease in the mitochondrial membrane potential in tumour cells, Furthermore, it downregulated the protein expression of active β-catenin and Cyclin D1, which are major target proteins of the Wnt signalling pathway, and reduced the expression of anti-apoptotic protein Bcl-xL. The combination of conditioned medium and sFRP4 further potentiated the effects, depending on the tumour cell line and experimental assay.

We conclude that factors derived from conditioned medium of adipose-derived mesenchymal stem cells and sFRP4 significantly decreased the tumour cell viability and migration rates (MCF-7), accompanied with an enhanced apoptotic activity through inhibition of canonical Wnt signalling. Besides giving an insight to possible paracrine interactions and influence of signalling pathways, reflective of a breast tumour microenvironment, this study emphasizes the utilization of cell free-secreted factors and Wnt antagonists to improve conventional anti-cancer strategies.

Keywords:

Adipose-derived mesenchymal stem cells; conditioned medium; breast cancer; Wnt signalling; secreted frizzled-related protein 4.

1. Introduction

Breast cancer is the most common cancer diagnosed in women worldwide and is the leading cause of cancer-related death in women (Jemal et al., 2011). In Australia, 1 in 8 women have had breast cancer by 85 years of age. Emerging evidence suggest that the tumour cells and non-tumour cells are components of a close-knit cellular network influencing the progression of tumour growth. Amongst the non-tumour cells, adipose-derived mesenchymal stem cells (ADSCs) are an important cell population present within breast adipose tissue (Karnoub et al., 2007; Liu et al., 2011; Martin et al., 2010; Molloy et al., 2009). Our study will provide important information on the crosstalk between ADSCs and tumour cells occurring within the breast tumour microenvironment.

The intrinsic inhibitory effect of mesenchymal stem cells (MSCs) on tumour growth has been demonstrated with respect to various tumour cell lines such as breast cancer (Clarke et al., 2015), glioblastoma (Dasari et al., 2010; Ho et al., 2013; Yang et al., 2014), liver cancer (Qiao, Xu, Zhao, Ye, & Zhang, 2008), pancreatic cancer (Kidd et al., 2010), prostate cancer, colon cancer (Ohlsson et al., 2003), myeloma (Ciavarella et al., 2012), sarcoma (Khakoo et al., 2006), and lymphoma (Secchiero et al., 2010). Some of the anti-tumour effects contributed by MSCs have been attributed to the secreted factors released by them (Madrigal, Rao, & Riordan, 2014). Conditioned medium derived from various sources of MSCs

demonstrated anti-tumour activity against various solid tumour types (Ahn et al., 2015; Cho et al., 2009; Cortes-Dericks et al., 2016; Ryu et al., 2014; Widowati et al., 2015). We examined the effect of secreted components present in the ADSC-conditioned medium (ADSC-CM) and their effect in combination with the Wnt antagonist secreted frizzled-related protein-4 (sFRP4) may generate enhanced anti-tumour activity in breast cancer cells.

Amongst the various signalling pathways that influence breast cancer progression, a Wnt signalling pathway is thought to play a key role (Gillett et al., 2001; Jang et al., 2015; Khramtsov et al., 2010; King et al., 2012; Lacroix-Triki et al., 2010; Lin et al., 2000; Lopez-Knowles et al., 2010; Xu et al., 2015). APC truncation accompanied with β-catenin upregulation has been reported in the breast cancer cell line DU-4475 (Schlosshauer et al., 2000). Since Wnt signalling and Wnt antagonists play a key role in cancer progression, we hypothesised that inhibition of Wnt signalling using the Wnt antagonist secreted frizzled-related protein 4 (sFRP4) would render the breast cancer cells more sensitive to chemotherapy. SFRP4 has previously been demonstrated by our laboratory and other groups to possess pro-apoptotic, anti-angiogenic, and anti-tumorigenic properties, the loss of which has been attributed to an aggressive phenotype in several cancer models (Drake et al., 2003; Jacob et al., 2012; Lacher et al., 2003; Muley et al., 2010; Saran et al., 2012; Wolf et al., 1997). SFRP4 was also shown to inhibit oestradiol-mediated proliferation of MCF-7 breast tumour cells via inhibition of the Wnt signalling pathway (Berry et al., 2014; McLaren et al., 2014).

Therefore in our study, we have performed experiments to determine the effect of ADSC-CM on the various growth parameters of tumour cell lines, both in the presence and absence of sFRP4. We have also determined the effect of insoluble extracellular matrix derived from ADSCs on tumour cell viability. Results from these experiments may indicate the extent of

crosstalk that exists between the tumour cells and ADSCs under physiological conditions and the extent of Wnt pathway-mediated regulation on the crosstalk.

2. Materials and Methods

2.1. Cell Culture

ADSCs isolated from lipoaspirate of non-diabetic patients undergoing elective liposuction surgery were purchased from Lonza (Basel, Switzerland) and cultured in RPMI (Sigma-Aldrich, St. Louis, MO, USA) containing 10% heat-inactivated foetal bovine serum (FBS) (Bovogen Biologicals, Melbourne, VIC, Australia) and 1% Penicillin-Streptomycin (PS) antibiotics (Hyclone Laboratories Inc, South Logan, Utah, USA). Breast tumour cell lines MCF-7 and MDA MB-231 were purchased from ATCC and cultured in the same medium as above. All cell types were cultured at 37^{o}C in the presence of 5% CO_2. ADSCs were used within passages 2-8, whereas tumour cell lines were used at later passages >P10.

2.2 Harvest of conditioned medium from ADSCs (ADSC-CM)

ADSCs were cultured in T25 or T75 flasks to attain around 80% confluency, following which the growth medium containing 10% FBS was removed. The ADSCs were given 2 PBS washes and rinsed with serum-free RPMI. Following the washes, 4mL and 12mL of fresh serum-free RPMI containing 1% PS was added for conditioning into T25 and T75 flasks respectively. Initial screening of conditioned medium harvested at various time-points was undertaken for its effect on tumour cell viability. The conditioned medium obtained at 48 hr demonstrated maximum reduction in tumour cell viability, which will be hereafter abbreviated as ADSC-CM, and was utilised for subsequent assays. ADSC-CM was harvested for centrifugation at 2000g for 10 minutes, followed by membrane filtration (0.22µ filters) to remove any cell debris, and was used immediately at 100% concentration (undiluted) for further experiments.

2.3. Characterisation of ADSC-CM by molecular weight cut-off (MWCO) filtration

To characterise the ADSC-CM, we used molecular weight cut off (MWCO) filters to fractionate the <30kDa and >30kDa ADSC-CM fractions. 30kDa was selected as the cut-off point to determine if the sFRP4-containing fraction (sFRP4 molecular weight = 50kDa) of the ADSC-CM was responsible for the inhibitory effect observed. The flow-through of ADSC-CM obtained after filtration contained the <30kDa fraction and was used to perform cell viability assays to determine if this fraction still retained the inhibitory effect. Additionally, another set of molecular fractionation was also performed using the 3kDa MWCO filter, resulting in the <3kDa flow through and the >3 kDa retentate (reconstituted in equal volume of fresh serum-free RPMI) that was used to treat tumour cells to determine their effects on tumour cell viability.

2.4. Characterisation of ADSC-CM by inactivation of protein component of ADSC-CM

To determine whether the inhibitory effect of ADSC-CM was originating from the protein or non-protein component of the CM, it was subjected to denaturing conditions at 95^{o}C for 5 minutes and then ADSC-CM was cooled down to room temperature prior to its addition to the tumour cell lines. A cell viability assay was performed using the tumour cell lines to identify if the inhibitory effect was retained in the denatured heat-inactivated ADSC-CM (HI-ADSC-CM). Further, the protein component of ADSC-CM was inactivated by enzymatic methods using protease digestion (proteinase K, protease, and trypsin) followed by its inactivation using heat or chemical inhibitors such as the soybean trypsin inhibitor (STI).

2.5. Recombinant sFRP4 Protein

Recombinant sFRP4 protein (Cat No: 1875-SF-025 R&D Systems, Inc., Minneapolis, MN, USA) was exogenously added to the cells at a dose of 250pg/mL, which was previously

validated by our laboratory (Muley et al., 2010; Perumal et al., 2016; Warrier, Balu, Kumar, Millward, & Dharmarajan, 2013), and the treatment durations are as indicated for each experiment.

2.6. Cell viability assay for adherent cells

Cell viability was measured by absorption spectrophotometry using methyl thiazolyl tetrazolium (MTT) reagent (Sigma-Aldrich, St. Louis, MO, USA) at 5mg/mL concentration. Tumour cells were seeded at 5000 cells/well in a 96 well plate and left to adhere overnight onto the tissue culture-treated plate surface. On the next day, the growth medium was removed and respective treatments with ADSC-CM in the presence and absence of sFRP4 were performed for 24, 48, and 72 hr durations.

Alternatively, short overnight pre-treatments were performed using sFRP4, after which the medium was replaced with ADSC-CM or non-conditioned control medium to determine whether sFRP4 was able to sensitise the tumour cells to a subsequent ADSC-CM treatment. After the indicated treatments and durations, 10µL of MTT (5mg/mL) was added to 100µL medium for 4 hr incubation at 37^{o}C. The formed formazan crystals were dissolved in 100µL DMSO. The absorbance was measured at 555nm using a plate reader (Enspire multimode, Perkin Elmer, Waltham, MA, USA), and corresponded to the number of viable cells.

2.7. Migration assay

A scratch was made using a 200µL sterile tip on a 90% confluent well of tumour cells cultured in a 6 well plate and then rinsed with PBS to remove cell debris. Following this, respective treatments with ADSC-CM, HI-ADSC-CM, MWCO fractions of ADSC-CM, and co-treatment with sFRP4 were performed and images of the scratch were captured using an inverted microscope (Nikon Instruments Inc, Melville, NY, USA) before and after treatment

at 0 hr (T0) and 24 hr (T24). The width of the gap was measured at T0 and T24 using Image J software, and the distance migrated was calculated using T0-T24. Further, to confirm the effect of ADSC-CM on solely the migratory activity, mitomycin-C (MMC) treatment was performed prior to treatment with ADSC-CM.

2.8. Mitochondrial membrane depolarisation assay

A JC1 assay was performed to detect early events of apoptosis occurring after treatment with ADSC-CM on the tumour cell lines. Briefly, after 72 hr treatment of tumour cells with ADSC-CM in the presence and absence of sFRP4 in a black 96 well plate, the medium was replaced with fresh medium and the JC1 dye (Cayman Chemical, Ann Arbor, MI, USA) was added at 10µL/100µL of medium in a 96 well plate. The cells were incubated for 30 minutes at 37^{o}C. After the incubation period, the cells were centrifuged to remove the supernatant and then subjected to two washes with assay buffer to remove any excess unbound dye. Immediately after the washes, the fluorescence emitted was measured using a plate reader (Enspire multimode, Perkin Elmer, Waltham, MA, USA). JC1 aggregates formed in healthy cells fluoresce red, and were detected by fluorescence with excitation/emission wavelengths of 535nm/595nm; the JC1 monomers present in apoptotic cells fluoresce green, and were detected at excitation/emission wavelengths of 485nm/535nm. A low red:green ratio is indicative of mitochondrial depolarisation, and hence, their entry into apoptosis.

2.9. Caspase 3/7 assay

Tumour cells were treated with ADSC-CM in the presence and absence of sFRP4 for 72 hr in a 6 well plate, and after treatment, the cells were harvested to prepare cell lysates. The assay was performed as per the manufacturer's instructions (Enzcheck® Caspase-3 Assay kit #2, Z-DEVD-R110 substrate; Thermo Fisher Scientific, Waltham, MA, USA). Briefly, cells were lysed and the lysate was centrifuged to remove cell debris. Following centrifugation, 50µL of

the cell lysate was transferred to a black 96 well plate and 50µL of 2X substrate working solution was added to the wells. The plate was incubated at room temperature for 30 minutes and the fluorescence emitted was measured using a plate reader (Perkin Elmer, Waltham, MA, USA) at excitation/emission wavelengths of 496nm/520nm respectively. The fluorescence emission corresponded to the levels of caspase 3/7 enzyme generation in the cells.

2.10. Western blot analysis

Tumour cells were plated in 6 well plates and respective treatments were performed with ADSC-CM in the presence and absence of sFRP4 for 72 hr. Following treatment, the cells were lifted with a cell scraper and centrifuged at 2000rpm for 5 minutes to obtain a cell pellet. After discarding the supernatant, the cell pellet was re-suspended in RIPA cell lysis buffer containing proteinase phosphatase inhibitor cocktail and 1mM phenylmethanesulfonyl fluoride. The protein concentration of cell lysate was measured by BCA Assay, and 10-15µg protein was loaded per lane of SDS-PAGE for immunoblotting. The proteins on the gel were transferred to a nitrocellulose membrane using a wet transfer protocol for 1 hr. The membrane was blocked at room temperature for 1 hr using 5% non-fat dry milk powder prepared in 1xPBS containing 0.1% Tween-20 (PBST). Primary antibodies at 1:1000 concentration (Cyclin D1, Bax, Bcl-xL, active β-catenin, and β-actin; Cell Signaling Technology, Danvers, MA, USA) were prepared in 5% bovine serum albumin in 1xPBST, and added to the membrane and left to incubate overnight on a shaker at 4^{o}C. Secondary antibody was added the next day at 1:2000 concentration and incubated for 1 hr at room temperature on a shaker. After blocking, primary antibody incubation, and secondary incubation steps, 4-5 washes (5 minutes each) were performed on the membrane using PBST. The membrane was developed using reagents for enhanced chemiluminescence and imaged

using the BioRad Gel Documentation system. The bands observed were quantitated by densitometry using the BioRad Image lab software.

2.11. Treatment with ADSC-derived extracellular matrix (ECM)

The ADSCs were seeded at confluent densities in a 96 well plate (10,000-15,000 cells/well) and were allowed to grow and secrete ECM for up to 3 days. On Day 3, the ADSCs were decellularised in order to obtain the ADSC-derived ECM. For decellularisation, the ADSCs were treated with 20mM ammonium hydroxide and 0.5% Triton-X 100 reagent for 2-3 minutes and thereafter rinsed thrice with ice-cold PBS to remove any cell debris. Decellularisation was confirmed by performing DAPI staining.

After the decellularisation, the tumour cells were seeded (at 5000 cell/well) onto the ADSC-secreted ECM in a 96 well plate and allowed to grow on this matrix. As a control, tumour cells were grown on a normal tissue culture-treated surface. Treatments were performed in the presence and absence of sFRP4. MTT cell viability assay was performed as indicated above at the 72 hr time-point.

2.12 Data analysis

Experiments were performed in multiple biological replicates ($n \geq 3$). The mean values ± SEM were determined and the statistical significance was calculated using Student's t-test to compare between the values of treatment conditions against untreated controls (indicated by *) and between treatment groups (indicated by #). A p value of < 0.05 was considered to be statistically significant. The graphs were prepared using GraphPad Prism software, and Microsoft PowerPoint software was used to grayscale the images and to prepare the figures.

3. Results

3.1. Effect on cell viability of tumour cell lines

ADSC-CM decreased the cell viability of both breast tumour cell lines MCF-7 and MDA-MB-231 as indicated by the MTT cell viability assays after 24 hr, 48 hr, and 72 hr of treatment (Fig. 1). A dose response was also performed on both tumour cell lines using the undiluted and partially diluted ADSC-CM at different dilutions ranging from 100%, 75%, 50%, and 10% (Supplementary fig. 1). ADSC-CM was used at 100% undiluted concentration for all the assays. Further, we found that when the ADSC-CM was combined with exogenous addition of the Wnt antagonist sFRP4, it resulted in a significant further reduction in the cell viability across all 3 time-points in MCF-7 cells (Fig. 1). In MDA-MB-231 cells, a significant further reduction in their viability was observed when ADSC-CM was combined with sFRP4 treatment for 72 hr as compared to ADSC-CM alone (Fig. 1).

Apart from the 48 hr CM, which is referred to as ADSC-CM, conditioned medium was also harvested from ADSCs at other time-points such as after 3 hr, 12hr, and 24hr of conditioning and its effect on tumour cell viability was determined (Supplementary fig. 2).

3.2. Characterisation of ADSC-CM by molecular weight fractionation

The inhibitory effect elicited by ADSC-CM prompted us to investigate which components of the CM contributed to the effect. We performed molecular fractionation and heat denaturation studies to investigate the properties of ADSC-CM. We found that the inhibitory effect contributed by the whole ADSC-CM was retained in the <30kDa of the ADSC-CM (Fig. 2A) as well as within the <3kDa fraction (Supplementary fig. 3). However, the desalted ADSC-CM (reconstituted retentate containing the >3 kDa fraction) did not cause an inhibitory effect on tumour cells. The morphology of tumour cells treated with the MWCO filtration-fractions of ADSC-CM has been included in Supplementary fig. 4.

3.3. Characterisation of ADSC-CM by inactivation of its protein component

We also found that the reduction in cell viability of the tumour cells was still present when treated with denatured ADSC-CM (Fig. 2B). Altogether, these data suggest that ADSC-CM possesses anti-tumour activity in its low molecular weight (<30kDa and <3kDa) and heat stable fraction, and therefore is likely contributed by the non-protein component of the ADSC-CM. As seen in Supplementary fig. 5, protease treatment of ADSC-CM at various doses of protease enzyme still retained residual protease activity that resulted in detachment of adherent tumour cells from the tissue culture surface. However, trypsin at 1:20 concentration followed by its inactivation using STI at 400µg/mL was performed successfully and the results are shown in Supplementary fig. 6. The inhibitory activity was still retained in the trypsin-digested fraction of ADSC-CM as compared to trypsin-digested control medium on MDA-MB-231 cells (Supplementary fig. 6). The morphology of tumour cells treated with HI-ADSC-CM and protease/trypsin-digested ADSC-CM has been included in Supplementary fig. 4.

3.4. Effect on migration of tumour cell lines

In order to determine if the inhibitory activity of ADSC-CM extended towards other aspects of tumour growth such as tumour cell migration, we performed a scratch wound assay and measured the amount of gap closure following treatment with ADSC-CM. We found that the ADSC-CM had a significant effect on reducing the migratory ability of the MCF-7 cells (Fig. 3A and C) but not that of the MDA-MB-231 cells (Fig. 3B and C). Further, co-treatment of ADSC-CM with sFRP4 was also observed to decrease the migratory capacity of MCF-7 cells (Supplementary fig. 7). Moreover, the inhibitory activity of ADSC-CM was retained on MCF-7 cells when treated in the presence of HI-ADSC-CM as well as with <3kDa fraction of ADSC-CM (Supplementary fig. 8, 9). Such inhibitory effects were not observed in MDA MB

231 cells with co-treatment of ADSC-CM with sFRP4, HI-ADSC-CM, and <3kDa fraction of ADSC-CM. The inhibitory effects on MCF-7 migration were independent of its inhibitory effect on their cell viability, as the inhibition was retained even in the presence of mitomycin-C (Supplementary fig. 7, 8, 9).

3.5. Effect on the mitochondrial membrane potential of tumour cell lines

We tested the effect of ADSC-CM on the mitochondrial membrane potential of the tumour cell lines and found that ADSC-CM caused depolarisation in both tumour cell lines, detected by a dramatic reduction in the mitochondrial membrane potential in MDA-MB-231 cells when compared to MCF-7 cells (Fig. 4A). However, there was no further depolarisation when the tumour cell lines were exposed to any of the combination treatments involving ADSC-CM and sFRP4 (Fig. 4A).

3.6. Effect on the caspase 3/7 activity of tumour cell lines

After detecting mitochondrial depolarisation upon treatment with ADSC-CM, we investigated its effect on caspase 3/7 enzyme activity in the tumour cell lines. We found that the caspase 3/7 levels were significantly upregulated upon treatment with ADSC-CM in MCF-7 cell line whereas in MDA-MB-231 cell line, there was only a 6% increase in caspase 3/7 activity following ADSC-CM treatment (Fig. 4B). Caspase 3/7 activity was not further upregulated during combination treatments with sFRP4 in MCF-7 cell line, whereas there was a 15% increase observed in MDA MB2 31 cell line following combination treatment of ADSC-CM with sFRP4 (Fig. 4B). Between the two tumour cell lines, it needs to be noted that the caspase 3/7 levels were higher in MCF-7 cells compared to MDA-MB-231 cells.

3.7. Effect on protein expression of tumour cell lines

To further investigate the effect of ADSC-CM on tumour cells, we performed protein expression profiling for proteins involved in Wnt signalling, proliferation, and apoptosis. We found that ADSC-CM, sFRP4, and the combination of ADSC-CM and sFRP4 were effective in decreasing the active β-catenin levels in both tumour cell lines after 72 hr treatment (Fig. 5A, B). A further significant reduction in active β-catenin was observed only in MCF-7 cells when a combination of ADSC-CM and sFRP4 was used (Fig. 5A). We also measured the levels of the apoptosis-associated proteins Bax and Bcl-xL and found that the levels of Bcl-xL were significantly reduced with ADSC-CM, sFRP4, and after combination treatments in MCF-7 and MDA-MB-231 cells (Fig. 5C, D). There was also an increasing trend (but statistically insignificant) observed in Bax protein expression with the treatments in both tumour cell lines (Data not shown). To determine the effect of ADSC-CM on a Wnt target gene involved in proliferation, we conducted Western blotting the levels of cyclin D1 protein expression. We detected a decrease in Cyclin D1 levels in MCF-7 cells with the ADSC-CM, sFRP4, and the combination treatments (Fig. 6A). In the MDA-MB-231 cell line, there was a decrease (statistically insignificant) in Cyclin D1 levels with ADSC-CM treatment alone, which decreased significantly following sFRP4 treatment (Fig. 6B). However, the combination treatment using ADSC-CM and sFRP4 did not further decrease the Cyclin D1 level in MDA-MB-231 cells (Fig. 6B).

3.8. Effect of ADSC-Extracellular Matrix (ADSC-ECM) on tumour cell viability

We observed a decrease in cell viability of the tumour cells when grown on the surface coated with extracellular matrix derived from ADSCs (Fig. 7A). A reduction in cell viability was seen in both tumour cell lines at the 72 hr time-point (measured using MTT cell viability assay). When tumour cells were exposed to a combination treatment, i.e. grown on ADSC-

ECM surface and supplemented with sFRP4, there was no further upregulation in the inhibitory activity as compared to ADSC-ECM treatment alone (Fig. 7A).

4. Discussion

MSCs are gaining much clinical attention for their potential applications in regenerative medicine and cell-based therapies. The clinical applications of MSCs in developing novel anti-cancer therapeutics are based on their tumour-specific homing property, followed by either exploiting their inherent anti-tumour properties (Dasari et al., 2010; Ho et al., 2013; Khakoo et al., 2006; Kidd et al., 2010; Ohlsson et al., 2003; Qiao et al., 2008; Secchiero et al., 2010) or by utilising their potency to be used as vehicles for delivery of anti-cancer agents at the tumour site (J. o. Ahn et al., 2013; Cavarretta et al., 2010; Ciavarella et al., 2012; Kucerova, Altanerova, Matuskova, Tyciakova, & Altaner, 2007; Kucerova et al., 2008; M. Studeny et al., 2002; Matus Studeny et al., 2004). A previous study also demonstrated MSCs as a delivery vehicle for the Wnt antagonist sFRP2, which successfully inhibited regrowth of castrate-resistant prostate cancer (Placencio, et al., 2010). Compared to other sources of MSCs, those derived from human fat (ADSCs) possess the distinct advantages of being easily accessible, requiring only minimally invasive surgery, and having higher proliferation rates (Li et al., 2015), which further facilitate their use in anti-cancer therapies.

Since ADSCs are the closest possible source of MSCs present within the breast, they could be the first and major cell population interacting with breast tumour cells. Before considering ADSCs for clinical applications to target cancer, it is imperative to understand the interaction between naïve ADSCs and breast tumour cells. Hence, our study aimed to investigate if the ADSC-derived factors possessed any anti-tumour activity and to examine the signalling events associated with it.

Our study has demonstrated the anti-tumour activity of ADSC-CM on various aspects of breast tumour cell behaviour. First, we observed that ADSC-CM exhibited significant cytotoxic effects in MCF-7 and MDA-MB-231 cells. This is in accordance with previous studies demonstrating a decrease in tumour cell viability following treatment with ADSCs or factors derived from them (Cousin et al., 2009; Takahara et al., 2014; Yu et al., 2015). Furthermore, we observed that the combinatorial treatment using sFRP4 and ADSC-CM resulted in an improved cytotoxic effect on both tumour cell lines. Previous studies have reported the role of Wnt antagonists in reducing viability in various tumour types (Horvath et al., 2007; Kahlert et al., 2015; Saran et al., 2012). However, our study is the first to report the combined use of sFRP4 with ADSC-derived factors to target breast cancer.

Although CM derived from MSCs has demonstrated anti-tumour activity in various tumour cell lines, the nature of the anti-tumour component present within the CM remains unclear. Furthermore, other studies have reported an increase in tumour forming behaviours from paracrine activity of MSCs in different cancer models (Hung et al., 2007; Karnoub et al., 2007; Zhang et al., 2013). Hence, in the current study, we further investigated the anti-tumour effects contributed by ADSC-CM by studying the role of various components within the ADSC-CM responsible for their effect in two phenotypically different breast tumour cell lines. We observed that ADSC-CM retained its anti-tumour activity even in its low molecular weight fraction (<30kDa). A few reports suggest that low molecular weight biomolecules present within the CM derived from MSCs are responsible for their tumour inhibitory activity (Cortes-Dericks et al., 2016; Ryu et al., 2014). Further, we also performed the molecular fractionation of ADSC-CM using 3kDa MWCO filters and measured tumour cell viability in the presence of <3kDa and >3kDa ADSC-CM fractions. It was observed that the <3kDa fraction of ADSC-CM still retained the inhibitory activity while the >3kDa (retentate yielded after molecular fractionation reconstituted in serum-free RPMI at equal volumes as ADSC-

CM) did not impose an inhibition on tumour cell viability. This shows that the inhibitory activity of the ADSC-CM was retained within its <3kDa fraction. However, the presence of increasing salt concentrations in the ADSC-CM and its involvement in inducing cell death could not be excluded.

This led us to explore the metabolic profile of the anti-tumour components in order to elucidate whether it was a protein or a non-protein-based biomolecule. Our results showed that the cytotoxic effect of ADSC-CM was still retained on both tumour cell lines in spite of denaturing the protein components, making it clear that the effects were mediated by a non-protein component present within the ADSC-CM. Similar results were obtained on MDA-MB-231 cells when the protein components of ADSC-CM was digested using trypsin treatment followed by its inactivation using STI. The non-protein molecules secreted into the CM could be biomolecules belonging to the category of lipids, nucleic acids, microvesicles or exosomes, which needs to be further defined. Nonetheless, it could also be due to the retention of intrinsically disordered protein (IDP) molecules in the CM, which are unstructured proteins lacking an ordered three-dimensional structure even in non-denaturing conditions and merely possess an intact primary structure. Denaturation normally targets folded structures, and hence, IDPs could potentially survive denaturation and remain functionally active. A previous study suggests that IDPs account for 10% of the secreted proteins (Dirndorfer et al., 2013). However, it will need to be further elucidated if these molecules are secreted by ADSCs and whether they play a role in modulating the ADSC-CM activity.

Next, we determined whether the anti-tumour activity of ADSC-CM extended to other parameters of tumour growth. Since the migratory property of tumour cells forms the basis for their invasiveness and metastasis, we investigated the effect of ADSC-CM to combat it. We found that MCF-7 cells were highly responsive to ADSC-CM, its MWCO fractions, HI-

ADSC-CM, and their co-treatment with sFRP4 resulting in their reduced migratory activity (Fig. 3, and Supplementary figure 7, 8, 9), but surprisingly, the ADSC-CM as well as the other treatments groups did not have any effect on the MDA-MB-231 cells (Fig. 3). MDA-MB-231 cells belong to the category of triple negative breast cancer, which are known to be highly aggressive and invasive (Gordon et al., 2003; Hunakova et al., 2009; Nagaraja et al., 2006), thereby accounting for their superior migratory potential as compared to other breast tumour cell lines. The heightened metastatic ability of these cells could be attributed to their unresponsiveness to ADSC-CM, resulting in an unchanged migration rate.

Having observed a decrease in the cell viability of the tumour cell lines, we further explored the underlying mechanisms. We found that the ADSC-CM destabilised the apoptotic machinery of both tumour cell lines at various stages of apoptosis. Mitochondrial depolarisation is one of the initial events occurring during apoptosis, which in turn triggers a cascade of downstream events resulting in the eventual release of executioner caspase enzymes to effect cell death. While MCF-7 cells demonstrated a significant degree of depolarisation, it was induced to a higher magnitude in MDA-MB-231 cells in response to ADSC-CM treatment, as observed by a low mitochondrial membrane potential. Further, in both cell lines, comparing the combinatorial treatments involving ADSC-CM and sFRP4 with ADSC-CM alone, there was no further induction of mitochondrial depolarisation, although we observed a significant further reduction in cell viability. This suggests that when ADSC-CM and sFRP4 are combined, the mechanism through which cell viability was further reduced did not require increased mitochondrial depolarisation.

Since ADSC-CM was effective in turning on the apoptotic cascade, we wanted to explore its impact on the downstream event of apoptosis at the executioner level. Hence, we measured the generation of the effector caspases 3 and 7, which are the crucial mediators bringing about programmed cell death (McIlwain, Berger, & Mak, 2013). ADSC-CM increased the

generation of effector caspases in both tumour cell lines, but the increase was multiple folds higher in MCF-7 than in MDA-MB-231 cells. The difference in caspase activity between the two tumour cell lines could be due to MCF-7 being caspase-3 deficient (Jänicke, Sprengart, Wati, & Porter, 1998; Liang, Yan, & Schor, 2001), hence pushing the heightened activity of caspase 7.

Next, we wanted to determine the effect of our treatments on the protein expression of key proliferative and apoptosis markers. We found that ADSC-CM mediated its effects through the canonical Wnt signalling pathway, as demonstrated by a decrease in the active β-catenin protein levels in both cell lines. With the combination treatment of ADSC-CM and sFRP4, the further reduction in active β-catenin levels was significant in MCF-7 and not in MDA-MB-231 cells (Fig. 7A). The observation of inhibited canonical Wnt signalling could be correlated with a previous finding that demonstrated decreased tumour cell viability due to secretion of the Wnt antagonist Dkk1 by ADSCs, thereby mediating their anti-tumour activity through the canonical Wnt signalling pathway (Zhu et al., 2009). Also, MSCs derived from the human dermis of a dead foetus demonstrated a reduction in growth of breast tumour cells by secreting Dkk1 (Qiao et al., 2008). Cyclin D1 is a G1-phase cyclin involved in cell cycle progression from the G1 phase to S phase and is often deregulated in many cancer types (Musgrove, Caldon, Barraclough, Stone, & Sutherland, 2011). As expected, MCF-7 cells demonstrated a decrease in cyclin D1 (Fig. 6A), which may indicate an impaired re-entry to the cell cycle, and it corresponds with their decreased cell viability following ADSC-CM treatment. However, the unchanged levels of Cyclin D1 expression in the relatively more aggressive breast tumour cell line MDA-MB-231 cells after ADSC-CM treatment (Fig. 6B) could be considered as a feedback mechanism put forth by the cells to exit the G1 phase and attempting to re-enter the cell cycle. However, in these cells, the addition of sFRP4 along with ADSC-CM was able to lower the levels of Cyclin D1, which is a major target gene of β-

catenin mediated transcription (Ghoshal & Ghosh, 2016; Warrier et al., 2013). The significant downregulating effect of ADSC-CM and in its combination with sFRP4 in decreasing the levels of the anti-apoptotic protein Bcl-xL in both tumour cell lines could be correlated to the decreased cell viability findings (Beenken & Bland, 2002).

Extending our study briefly beyond the range of soluble factors secreted through the ADSC-CM, we also examined the effect of ADSC-ECM on the tumour cell lines. Our observations demonstrated that the insoluble components secreted by ADSCs into their ECM inhibited the cell viability of the tumour cells. At the 72 hr time-point, the ADSC-ECM induced strong inhibition on the tumour cells, which however, could not be further enhanced in the presence of sFRP4. There has been no previous research reporting the effect of ECM derived from MSCs on tumour cell growth, except for one study that demonstrated reduced cell viability in MDA-MB-231 cells, which corroborates our observation (Sun et al., 2010). However, our study is the first to identify the anti-tumour effect of ADSC-ECM in the presence and absence of sFRP4 on two phenotypically diverse breast tumour cell lines.

5. Conclusions

Overall, our study indicates that the non-protein component present in the low molecular weight fraction of the ADSC-CM was able to induce potent anti-tumour effects on biologically different subtypes of breast tumour cell lines. Further, ADSC-CM exhibited a strong antagonising effect on various aspects of tumour behaviour mediated through reduction of the canonical Wnt signalling pathway and Bcl-xL expression. The clinical potential of developing novel therapeutic strategies utilising the anti-tumour property of ADSC-derived secreted factors and Wnt antagonists need to be carefully considered. Furthermore, ADSCs could be harnessed to transport anti-cancer biomolecules such as Wnt antagonists, as used in a previous study where MSCs harboured sFRP2 to target castrate-

resistant prostate cancer (Placencio et al., 2010). Hence, the clinical inference of our study emphasises the possible therapeutic options utilising the anti-tumour potential of secreted factors derived from ADSCs and sFRP4.

Acknowledgements

We acknowledge the research and technical support from the School of Biomedical Sciences and Curtin Health Innovation Research Institute (CHIRI), Curtin University, where the work was carried out. MV is supported by scholarship from the Office of Research and Development, Faculty of Health sciences, Curtin University. AD is supported by strategic research funds from the School of Biomedical Sciences (Curtin University), Commercialisation Advisory Board of Curtin University, Cancer Council of Western Australia and Actinogen Ltd, Perth, Western Australia.

References

Ahn, J. O., Coh, Y. R., Lee, H. W., Shin, I. S., Kang, S. K., & Youn, H. Y. 2015. Human Adipose Tissue-derived Mesenchymal Stem Cells Inhibit Melanoma Growth In Vitro and In Vivo. Anticancer Research. 35 (1), 159-168.

Ahn, J. O., Lee, H. W., Seo, K. W., Kang, S. K., Ra, J. C., & Youn, H. Y. 2013. Anti-Tumor Effect of Adipose Tissue Derived-Mesenchymal Stem Cells Expressing Interferon-β and Treatment with Cisplatin in a Xenograft Mouse Model for Canine Melanoma. Plos one. 8 (9), e74897. doi:10.1371/journal.pone.0074897

Beenken, S. W., & Bland, K. I. 2002. Biomarkers for breast cancer. Minerva Chir. 57 (4), 437-448.

Berry, C., Charles, A. K., Zeps, N., Cregan, M., Arfuso, F., & Dharmarajan, A. 2014. Expression Profile of Wnt/b-Catenin Signalling Molecules and the Wnt Antagonist Secreted

Frizzled-Related Protein 4 in Apoptosis in Breast Cancer Tissue Micro-Arrays. J Anal Oncol. 3, 205-212.

Cavarretta, I. T., Altanerova, V., Matuskova, M., Kucerova, L., Culig, Z., & Altaner, C. 2010. Adipose tissue-derived mesenchymal stem cells expressing prodrug-converting enzyme inhibit human prostate tumor growth. Mol Ther. 18 (1), 223-231. doi:10.1038/mt.2009.237

Cho, J. A., Park, H., Kim, H. K., Lim, E. H., Seo, S. W., Choi, J. S., & Lee, K. W. 2009. Hyperthermia-treated mesenchymal stem cells exert antitumor effects on human carcinoma cell line. Cancer. 115 (2), 311-323. doi:10.1002/cncr.24032

Ciavarella, S., Grisendi, G., Dominici, M., Tucci, M., Brunetti, O., Dammacco, F., & Silvestris, F. 2012. In vitro anti-myeloma activity of TRAIL-expressing adipose-derived mesenchymal stem cells. Br J Haematol. 157 (5), 586-598. doi:10.1111/j.1365-2141.2012.09082.x

Clarke, M. R., Imhoff, F. M., & Baird, S. K. 2015. Mesenchymal stem cells inhibit breast cancer cell migration and invasion through secretion of tissue inhibitor of metalloproteinase-1 and -2. Mol Carcinog. 54 (10), 1214-1219. doi:10.1002/mc.22178

Cortes-Dericks, L., Froment, L., Kocher, G., & Schmid, R. A. 2016. Human lung-derived mesenchymal stem cell-conditioned medium exerts in vitro antitumor effects in malignant pleural mesothelioma cell lines. Stem Cell Research & Therapy. 7, 25. doi:10.1186/s13287-016-0282-7

Cortes-Dericks, L., Froment, L., Kocher, G., & Schmid, R. A. 2009. Adult Stromal Cells Derived from Human Adipose Tissue Provoke Pancreatic Cancer Cell Death both In Vitro and In Vivo. Plos one. 4 (7), e6278. doi:10.1371/journal.pone.0006278

Dasari, V. R., Kaur, K., Velpula, K. K., Gujrati, M., Fassett, D., Klopfenstein, J. D., et al., 2010. Upregulation of PTEN in Glioma Cells by Cord Blood Mesenchymal Stem Cells

Inhibits Migration via Downregulation of the PI3K/Akt Pathway. Plos one. 5 (4), e10350. doi:10.1371/journal.pone.0010350

Dirndorfer, D., Seidel, R. P., Nimrod, G., Miesbauer, M., Ben-Tal, N., Engelhard, M., et al., 2013. The α-Helical Structure of Prodomains Promotes Translocation of Intrinsically Disordered Neuropeptide Hormones into the Endoplasmic Reticulum. The Journal of Biological Chemistry. 288 (20), 13961-13973. doi:10.1074/jbc.M112.430264

Drake, J. M., Friis, R. R., & Dharmarajan, A. M. 2003. The role of sFRP4, a secreted frizzled-related protein, in ovulation. Apoptosis. 8 (4), 389-397.

Ghoshal, A., & Ghosh, S. S. 2016. Antagonizing canonical Wnt signaling pathway by recombinant human sFRP4 purified from E. coli and its implications in cancer therapy. Mol Cell Biochem. 418 (1-2), 119-135. doi:10.1007/s11010-016-2738-6

Gillett, C. E., Miles, D. W., Ryder, K., Skilton, D., Liebman, R. D., Springall, R. J., . . . Hanby, A. M. 2001. Retention of the expression of E-cadherin and catenins is associated with shorter survival in grade III ductal carcinoma of the breast. The Journal of Pathology. 193 (4), 433-441. doi:10.1002/path.831

Gordon, L. A., Mulligan, K. T., Maxwell-Jones, H., Adams, M., Walker, R. A., & Jones, J. L. 2003. Breast cell invasive potential relates to the myoepithelial phenotype. Int J Cancer. 106 (1), 8-16. doi:10.1002/ijc.11172

Ho, I. A., Toh, H. C., Ng, W. H., Teo, Y. L., Guo, C. M., Hui, K. M., & Lam, P. Y. 2013. Human bone marrow-derived mesenchymal stem cells suppress human glioma growth through inhibition of angiogenesis. Stem Cells. 31 (1), 146-155.

Horvath, L. G., Lelliott, J. E., Kench, J. G., Lee, C. S., Williams, E. D., Saunders, D. N., . . . Henshall, S. M. 2007. Secreted frizzled-related protein 4 inhibits proliferation and metastatic potential in prostate cancer. Prostate. 67 (10), 1081-1090.

Hunakova, L., Sedlakova, O., Cholujova, D., Gronesova, P., Duraj, J., & Sedlak, J. 2009. Modulation of markers associated with aggressive phenotype in MDA-MB-231 breast carcinoma cells by sulforaphane. Neoplasma. 56 (6), 548-556.

Hung, S., Pochampally, R., Chen, S., Hsu, S., & Prockop, D. 2007. Angiogenic effects of human multipotent stromal cell conditioned medium activate the PI3K-Akt pathway in hypoxic endothelial cells to inhibit apoptosis, increase survival, and stimulate angiogenesis. Stem Cells. 9, 2363 - 2370.

Jacob, F., Ukegjini, K., Nixdorf, S., Ford, C. E., Olivier, J., Caduff, R., et al., 2012. Loss of Secreted Frizzled-Related Protein 4 Correlates with an Aggressive Phenotype and Predicts Poor Outcome in Ovarian Cancer Patients. Plos one. 7 (2), e31885. doi:10.1371/journal.pone.0031885

Jang, G.-B., Kim, J.-Y., Cho, S.-D., Park, K.-S., Jung, J.-Y., Lee, H.-Y., et al., 2015. Blockade of Wnt/β-catenin signaling suppresses breast cancer metastasis by inhibiting CSC-like phenotype. Sci Rep. 5, 12465. doi:10.1038/srep12465 http://www.nature.com/articles/srep12465#supplementary-information

Jänicke, R. U., Sprengart, M. L., Wati, M. R., & Porter, A. G. 1998. Caspase-3 Is Required for DNA Fragmentation and Morphological Changes Associated with Apoptosis. Journal of Biological Chemistry. 273 (16), 9357-9360. doi:10.1074/jbc.273.16.9357

Jemal, A., Bray, F., Center, M. M., Ferlay, J., Ward, E., & Forman, D. 2011. Global cancer statistics. CA Cancer J Clin. 61(2), 69-90. doi:10.3322/caac.20107

Kahlert, U. D., Suwala, A. K., Koch, K., Natsumeda, M., Orr, B. A., Hayashi, M., et al., 2015. Pharmacological WNT Inhibition Reduces Proliferation, Survival and Clonogenicity of Glioblastoma Cells. Journal of neuropathology and experimental neurology. 74 (9), 889-900. doi:10.1097/NEN.0000000000000227

Karnoub, A., Dash, A., Vo, A., Sullivan, A., Brooks, M., Bell, G., et al., 2007. Mesenchymal stem cells within tumour stroma promote breast cancer metastasis. Nature, 7162, 557 - 563.

Khakoo, A., Pati, S., Anderson, S., Reid, W., Elshal, M., Rovira, I., et al., 2006. Human mesenchymal stem cells exert potent antitumorigenic effects in a model of Kaposi's sarcoma. J Exp Med. 5, 1235 - 1247.

Khramtsov, A. I., Khramtsova, G. F., Tretiakova, M., Huo, D., Olopade, O. I., & Goss, K. H. 2010. Wnt/β-Catenin Pathway Activation Is Enriched in Basal-Like Breast Cancers and Predicts Poor Outcome. The American Journal of Pathology. 176 (6), 2911-2920. doi:10.2353/ajpath.2010.091125

Kidd, S., Caldwell, L., Dietrich, M., Samudio, I., Spaeth, E. L., Watson, K., et al., 2010. Mesenchymal stromal cells alone or expressing interferon-beta suppress pancreatic tumors in vivo, an effect countered by anti-inflammatory treatment. Cytotherapy. 12 (5), 615-625. doi:10.3109/14653241003631815

King, T. D., Suto, M. J., & Li, Y. 2012. The Wnt/beta-catenin signaling pathway: a potential therapeutic target in the treatment of triple negative breast cancer. J Cell Biochem. 113 (1), 13-18. doi:10.1002/jcb.23350

Kucerova, L., Altanerova, V., Matuskova, M., Tyciakova, S., & Altaner, C. 2007. Adipose tissue-derived human mesenchymal stem cells mediated prodrug cancer gene therapy. Cancer Res. 67 (13), 6304-6313. doi:10.1158/0008-5472.can-06-4024

Kucerova, L., Matuskova, M., Pastorakova, A., Tyciakova, S., Jakubikova, J., Bohovic, R., et al., 2008. Cytosine deaminase expressing human mesenchymal stem cells mediated tumour regression in melanoma bearing mice. J Gene Med. 10 (10), 1071-1082. doi:10.1002/jgm.1239

Lacher, M. D., Siegenthaler, A., Jager, R., Yan, X., Hett, S., Xuan, L., et al., 2003. Role of DDC-4//sFRP-4, a secreted Frizzled-related protein, at the onset of apoptosis in mammary involution. Cell Death Differ. 10 (5), 528-538.

Lacroix-Triki, M., Geyer, F. C., Lambros, M. B., Savage, K., Ellis, I. O., Lee, A. H., & Reis-Filho, J. S. 2010. beta-catenin/Wnt signalling pathway in fibromatosis, metaplastic carcinomas and phyllodes tumours of the breast. Mod Pathol. 23(11), 1438-1448. doi:10.1038/modpathol.2010.141

Li, C. Y., Wu, X. Y., Tong, J. B., Yang, X. X., Zhao, J. L., Zheng, Q. F., et al., 2015. Comparative analysis of human mesenchymal stem cells from bone marrow and adipose tissue under xeno-free conditions for cell therapy. Stem Cell Res Ther. 6, 55. doi:10.1186/s13287-015-0066-5

Liang, Y., Yan, C., & Schor, N. F. 2001. Apoptosis in the absence of caspase 3. Oncogene. 20 (45), 6570-6578. doi:10.1038/sj.onc.1204815

Lin, S. Y., Xia, W., Wang, J. C., Kwong, K. Y., Spohn, B., Wen, Y., et al., 2000. Beta-catenin, a novel prognostic marker for breast cancer: its roles in cyclin D1 expression and cancer progression. Proc Natl Acad Sci U S A. 97 (8), 4262-4266.

Liu, S., Ginestier, C., Ou, S. J., Clouthier, S. G., Patel, S. H., Monville, F., et al., 2011. Breast Cancer Stem Cells Are Regulated by Mesenchymal Stem Cells through Cytokine Networks. Cancer Research. 71 (2), 614-624. doi:10.1158/0008-5472.can-10-0538

Lopez-Knowles, E., Zardawi, S. J., McNeil, C. M., Millar, E. K., Crea, P., Musgrove, E. A., et al., 2010. Cytoplasmic localization of beta-catenin is a marker of poor outcome in breast cancer patients. Cancer Epidemiol Biomarkers Prev. 19 (1), 301-309. doi:10.1158/1055-9965.epi-09-0741

Madrigal, M., Rao, K. S., & Riordan, N. H. 2014. A review of therapeutic effects of mesenchymal stem cell secretions and induction of secretory modification by different

culture methods. Journal of Translational Medicine. 12 (1), 260. doi:10.1186/s12967-014-0260-8

Martin, F., Dwyer, R., Kelly, J., Khan, S., Murphy, J., Curran, C., et al., 2010. Potential role of mesenchymal stem cells (MSCs) in the breast tumour microenvironment: stimulation of epithelial to mesenchymal transition (EMT). Breast Cancer Res Treat. 2, 317 - 326.

McIlwain, D. R., Berger, T., & Mak, T. W. 2013. Caspase Functions in Cell Death and Disease. Cold Spring Harbor Perspectives in Biology. 5 (4). doi:10.1101/cshperspect.a008656

McLaren, S., Arfuso, F., Zeps, N., & Dhrmarajan, A. 2014. The role of secreted frizzled related protein 4 (sFRP-4) in regulating oestradiol-induced growth of the MCF-7 breast cancer cell line. J Anal Oncol. 3 (1), 1-10.

Molloy, A. P., Martin, F. T., Dwyer, R. M., Griffin, T. P., Murphy, M., Barry, F. P., et al., 2009. Mesenchymal stem cell secretion of chemokines during differentiation into osteoblasts, and their potential role in mediating interactions with breast cancer cells. Int J Cancer. 124 (2), 326-332. doi:10.1002/ijc.23939

Muley, A., Majumder, S., Kolluru, G. K., Parkinson, S., Viola, H., Hool, L., et al., 2010. Secreted frizzled-related protein 4: an angiogenesis inhibitor. Am J Pathol. 176 (3), 1505-1516.

Musgrove, E. A., Caldon, C. E., Barraclough, J., Stone, A., & Sutherland, R. L. 2011. Cyclin D as a therapeutic target in cancer. Nat Rev Cancer. 11 (8), 558-572.

Nagaraja, G. M., Othman, M., Fox, B. P., Alsaber, R., Pellegrino, C. M., Zeng, Y., et al., 2006. Gene expression signatures and biomarkers of noninvasive and invasive breast cancer cells: comprehensive profiles by representational difference analysis, microarrays and proteomics. Oncogene. 25 (16), 2328-2338. doi:10.1038/sj.onc.1209265

Ohlsson, L. B., Varas, L., Kjellman, C., Edvardsen, K., & Lindvall, M. 2003. Mesenchymal progenitor cell-mediated inhibition of tumor growth in vivo and in vitro in gelatin matrix. Exp Mol Pathol. 75 (3), 248-255.

Perumal, V., Pohl, S., Keane, K. N., Arfuso, F., Newsholme, P., Fox, S., & Dharmarajan, A. 2016. Therapeutic approach to target mesothelioma cancer cells using the Wnt antagonist, secreted frizzled-related protein 4: Metabolic state of cancer cells. Exp Cell Res. 341 (2), 218-224. doi:10.1016/j.yexcr.2016.02.008

Placencio, V. R., Li, X., Sherrill, T. P., Fritz, G., & Bhowmick, N. A. 2010. Bone Marrow Derived Mesenchymal Stem Cells Incorporate into the Prostate during Regrowth. Plos one. 5 (9), e12920. doi:10.1371/journal.pone.0012920

Qiao, L., Xu, Z.-l., Zhao, T.-j., Ye, L.-h., & Zhang, X.-d. 2008. Dkk-1 secreted by mesenchymal stem cells inhibits growth of breast cancer cells via depression of Wnt signalling. Cancer Letters. 269 (1), 67-77. doi:http://dx.doi.org/10.1016/j.canlet.2008.04.032

Ryu, H., Oh, J. E., Rhee, K. J., Baik, S. K., Kim, J., Kang, S. J., et al., 2014. Adipose tissue-derived mesenchymal stem cells cultured at high density express IFN-beta and suppress the growth of MCF-7 human breast cancer cells. Cancer Lett. 352 (2), 220-227. doi:10.1016/j.canlet.2014.06.018

Saran, U., Arfuso, F., Zeps, N., & Dharmarajan, A. 2012. Secreted frizzled-related protein 4 expression is positively associated with responsiveness to Cisplatin of ovarian cancer cell lines in vitro and with lower tumour grade in mucinous ovarian cancers. BMC Cell Biology. 13 (1), 25.

Schlosshauer, P. W., Brown, S. A., Eisinger, K., Yan, Q., Guglielminetti, E. R., Parsons, R., . . . Kitajewski, J. 2000. APC truncation and increased beta-catenin levels in a human breast cancer cell line. Carcinogenesis. 21 (7), 1453-1456.

Secchiero, P., Zorzet, S., Tripodo, C., Corallini, F., Melloni, E., Caruso, L., et al., 2010. Human Bone Marrow Mesenchymal Stem Cells Display Anti-Cancer Activity in SCID Mice Bearing Disseminated Non-Hodgkin's Lymphoma Xenografts. Plos one. 5 (6), e11140. doi:10.1371/journal.pone.0011140

Studeny, M., Marini, F. C., Champlin, R. E., Zompetta, C., Fidler, I. J., & Andreeff, M. 2002. Bone marrow-derived mesenchymal stem cells as vehicles for interferon-beta delivery into tumors. Cancer Res. 62 (13), 3603-3608.

Studeny, M., Marini, F. C., Dembinski, J. L., Zompetta, C., Cabreira-Hansen, M., Bekele, B. N., . . . Andreeff, M. 2004. Mesenchymal Stem Cells: Potential Precursors for Tumor Stroma and Targeted-Delivery Vehicles for Anticancer Agents. Journal of the National Cancer Institute. 96 (21), 1593-1603. doi:10.1093/jnci/djh299

Sun, B., Yu, K. R., Bhandari, D. R., Jung, J. W., Kang, S. K., & Kang, K. S. 2010. Human umbilical cord blood mesenchymal stem cell-derived extracellular matrix prohibits metastatic cancer cell MDA-MB-231 proliferation. Cancer Lett. 296 (2), 178-185. doi:10.1016/j.canlet.2010.04.007

Takahara, K., Ii, M., Inamoto, T., Komura, K., Ibuki, N., Minami, K., et al., 2014. Adipose-derived stromal cells inhibit prostate cancer cell proliferation inducing apoptosis. Biochem Biophys Res Commun. 446 (4), 1102-1107. doi:10.1016/j.bbrc.2014.03.080

Warrier, S., Balu, S. K., Kumar, A. P., Millward, M., & Dharmarajan, A. 2013. Wnt antagonist, secreted frizzled-related protein 4 (sFRP4), increases chemotherapeutic response of glioma stem-like cells. Oncol Res. 21 (2), 93-102. doi:10.3727/096504013x13786659070154

Widowati, W., Wijaya, L., Murti, H., Widyastuti, H., Agustina, D., Laksmitawati, D. R., et al., 2015. Conditioned medium from normoxia (WJMSCs-norCM) and hypoxia-treated

WJMSCs (WJMSCs-hypoCM) in inhibiting cancer cell proliferation. Biomarkers and Genomic Medicine. 7 (1), 8-17. doi:http://dx.doi.org/10.1016/j.bgm.2014.08.008

Wolf, V., Ke, G., Dharmarajan, A. M., Bielke, W., Artuso, L., Saurer, S., & Friis, R. 1997. DDC-4, an apoptosis-associated gene, is a secreted frizzled relative. FEBS Letters. 417 (3), 385-389. doi:http://dx.doi.org/10.1016/S0014-5793(97)01324-0

Xu, J., Prosperi, J. R., Choudhury, N., Olopade, O. I., & Goss, K. H. 2015. β-Catenin Is Required for the Tumorigenic Behavior of Triple-Negative Breast Cancer Cells. Plos one. 10 (2), e0117097. doi:10.1371/journal.pone.0117097

Yang, C., Lei, D., Ouyang, W., Ren, J., Li, H., Hu, J., & Huang, S. 2014. Conditioned Media from Human Adipose Tissue-Derived Mesenchymal Stem Cells and Umbilical Cord-Derived Mesenchymal Stem Cells Efficiently Induced the Apoptosis and Differentiation in Human Glioma Cell Lines In Vitro. BioMed Research International. 2014, 109389. doi:10.1155/2014/109389

Yu, X., Su, B., Ge, P., Wang, Z., Li, S., Huang, B., et al., 2015. Human Adipose Derived Stem Cells Induced Cell Apoptosis and S Phase Arrest in Bladder Tumor. Stem Cells International. 2015, 12. doi:10.1155/2015/619290

Zhang, T., Lee, Y., Rui, Y., Cheng, T., Jiang, X., & Li, G. 2013. Bone marrow-derived mesenchymal stem cells promote growth and angiogenesis of breast and prostate tumors. Stem Cell Research & Therapy. 4 (3), 70.

Zhu, Y., Sun, Z., Han, Q., Liao, L., Wang, J., Bian, C., et al., 2009. Human mesenchymal stem cells inhibit cancer cell proliferation by secreting DKK-1. Leukemia. 23 (5), 925-933.

Figure Legends

Fig. 1. Cell Viability of tumour cell lines after conditioned medium-derived from adipose-derived mesenchymal stem cells (ADSC-CM) treatment measured by methyl thiazolyl tetrazolium cell viability assay. MCF-7 and MDA-MB-231 cells (0.005 x 10^6 cells/well) were treated with ADSC-CM in the presence and absence of sFRP4 for (A) 24 hr, (B) 48 hr, and (C) 72 hr durations. * $p<0.05$ versus untreated control, #$p<0.05$ between treatment groups.

Fig. 2. Characterisation of conditioned medium-derived from adipose-derived mesenchymal stem cells (ADSC-CM) and its effect on tumour cell viability measured using methyl thiazolyl tetrazolium cell viability assay. MCF-7 and MDA-MB-231 cells (0.005 x 10^6 cells/well) were treated with ADSC-CM obtained after molecular fractionation and denaturation studies for 72 hr. (A) Effect of whole ADSC-CM and <30kDa fraction of ADSC-CM on the viability of tumour cell lines. (B) Effect of non-denatured ADSC-CM and heat denatured ADSC-CM on tumour cell viability. *$p<0.05$ versus untreated control, #$p<0.05$ between treatment groups.

Fig. 3. Migratory potential of tumour cell lines measured by distance migrated using a scratch wound assay. MCF-7 and MDA-MB-231 cells were seeded at confluent densities and treated with conditioned medium-derived from adipose-derived mesenchymal stem cells (ADSC-CM) for 24 hr. (A) Wound healing assay performed on MCF-7 cells (Scale bar = 100µm). (B) Wound healing assay performed on MDA-MB-231 cells (Scale bar = 100µm). (C) Migratory potential of MCF-7 and MDA-MB-231 cells following treatment with ADSC-CM for 24 hr performed using a scratch wound healing assay. *$p<0.05$ versus untreated control.

Fig. 4. Measurement of mitochondrial membrane potential and caspase activity (A) Measurement of mitochondrial membrane potential using JC1 assay. MCF-7 and MDA-MB-

231 cells (0.05 x 10^6 cells/well) were treated with conditioned medium-derived from adipose-derived mesenchymal stem cells (ADSC-CM) in the presence and absence of sFRP4 for 72 hr. Ratio of JC1 aggregates/JC1 monomers is used as an indicator of cell death, with a lower ratio indicating more cell death. (B) Measurement of caspase 3/7 enzyme activity. MCF-7 and MDA-MB-231 cells (~ 1 x 10^6 cells/well) were treated with ADSC-CM in the presence and absence of sFRP4 for 72 hr. *$p<0.05$ versus untreated control.

Fig. 5. Protein expression of active β-catenin and Bcl-xL. MCF-7 and MDA-MB-231 cells were seeded in 6 well plates or 24 well plates and treated with conditioned medium-derived from adipose-derived mesenchymal stem cells (ADSC-CM) in the presence and absence of sFRP4 for 72 hr. Effect of treatments on protein expression of active β-catenin in (A) MCF-7. (B) MDA-MB-231tumour cell lines, and Bcl-xL in (C) MCF-7 (D) MDA-MB-231 tumour cell lines. (E) Representative blot images (ADSC-CM indicated as CM). *$p<0.05$ versus untreated control, #$p<0.05$ between treatment groups.

Fig. 6. Expression of Cyclin D1. MCF-7 and MDA-MB-231 cells were seeded in 6 well plates or 24 well plates and treated with conditioned medium-derived from adipose-derived mesenchymal stem cells (ADSC-CM) in the presence and absence of sFRP4 for 72 hr. Effect of treatments on protein expression of Cyclin D1 in (A) MCF-7 and (B) MDA-MB-231 tumour cell lines. (C) Representative blot images . *$p<0.05$ versus untreated control.

Fig. 7. Cell Viability of tumour cell lines after extracellular matrix-derived from adipose-derived mesenchymal stem cells (ADSC-ECM) treatment measured by methyl thiazolyl tetrazolium cell viability assay. MCF-7 and MDA-MB-231 cells (0.005 x 10^6 cells/well) were cultured on ADSC-ECM in the presence and absence of sFRP4 for 72 hr. (A) Effect of ADSC-ECM in the presence and absence of sFRP4 on the viability of tumour cell

lines. (B) Microscopic observation of non-decellularised ADSCs and decellularised ADSCs after DAPI staining (Scale bar = 100μm) *p<0.05 versus untreated control.

Supplementary Figure Legends

Supp. Fig. 1. Dose response of conditioned medium-derived from adipose-derived mesenchymal stem cells (ADSC-CM) on cell viability of tumour cell lines measured by methyl thiazolyl tetrazolium cell viability assay. MCF-7 and MDA-MB-231 cells (0.005 x 10^6 cells/well) were treated with different dilutions of conditioned medium-derived from adipose-derived mesenchymal stem cells (ADSC-CM) (100%, 75%, 50%, and 10% ADSC-CM) for 72 hr duration. * p<0.05 versus untreated control.

Supp. Fig. 2. Cell viability of tumour cell lines treated with different conditioned medium (CM) harvested from ADSCs, measured by methyl thiazolyl tetrazolium cell viability assay. CM was harvested at different durations of conditioning – 3hr, 12hr, and 24hr from ADSCs and applied to tumour cells for 72 hr duration. *p<0.05 versus untreated control, #p<0.05 between treatment groups.

Supp. Fig. 3. Effect of <3kDa fraction and desalted fraction of conditioned medium-derived from adipose-derived mesenchymal stem cells (ADSC-CM) on tumour cell viability measured by methyl thiazolyl tetrazolium cell viability assay. Effect of whole conditioned medium-derived from adipose-derived mesenchymal stem cells (ADSC-CM), <3kDa fraction of ADSC-CM, and the >3kDa fraction of ADSC-CM (desalted fraction) on the viability of tumour cell lines after 72 hr duration. *p<0.05 versus untreated control, #p<0.05 between treatment groups.

Supp. Fig. 4. Morphological observation of tumour cells following treatment with different fractions of conditioned medium-derived from adipose-derived mesenchymal

stem cells (ADSC-CM). (A) heat-inactivated-ADSC-CM (HI-ADSC-CM), (B) Molecular weight cut-off (MWCO) fraction of ADSC-CM, and (C) Trypsin-digested ADSC-CM after 72 hr treatment duration. Scale bar = 500µm.

Supp. Fig. 5. Morphological observation of tumour cells and optimisation of protease doses on conditioned medium-derived from adipose-derived mesenchymal stem cells (ADSC-CM) for its protein digestion. (A) Different doses of protease added to ADSC-CM to digest its protein components, which were then applied to tumour cells, (B) Different doses of trypsin added to ADSC-CM to digest its protein components, which were then applied to tumour cells, (C) Measurement of tumour cell viability at72 hr time-point performed for initial optimisation of doses of trypsin and soybean trypsin inhibitor (STI). Scale bar = 500µm.

Supp. Fig. 6. Cell viability of tumour cells after treatment with trypsin-digested conditioned medium-derived from adipose-derived mesenchymal stem cells (ADSC-CM) measured using methyl thiazolyl tetrazolium cell viability assay. Trypsin was added at 1:20 dilution followed by inactivation using soybean trypsin inhibitor (STI) at 400µg/mL, and cells were treated for 72 hr time-point after which cell viability was measured.

Supp. Fig. 7. Migratory potential of MCF-7 cells after co-treatment of conditioned medium-derived from adipose-derived mesenchymal stem cells (ADSC-CM) with sFRP4, measured by distance migrated using a scratch wound assay. MCF-7 cells were seeded at confluent densities and treated with ADSC-CM in the presence of 250pg/mL sFRP4 for 24 hr. (A) Wound healing assay performed on MCF-7 cells at 0hr and 24 hr time-points in the presence and absence of 2µg/mL Mitomycin-C (Scale bar = 500µm). (B) Migratory potential of MCF-7 cells measured following treatment with ADSC-CM ± sFRP4 for 24 hr. *$p<0.05$ versus untreated control. Scale bar = 500µm.

Supp. Fig. 8. Migratory potential of MCF-7 cells with heat-inactivated fraction of conditioned medium-derived from adipose-derived mesenchymal stem cells (HI-ADSC-CM) measured by distance migrated using a scratch wound assay. MCF-7 cells were seeded at confluent densities and treated with HI-ADSC-CM for 24 hr. (A) Wound healing assay performed on MCF-7 cells at 0hr and 24 hr time-points in the presence and absence of 2µg/mL Mitomycin-C (Scale bar = 500µm). (B) Migratory potential of MCF-7 cells measured following treatment with HI-ADSC-CM for 24 hr. *$p<0.05$ versus untreated control. Scale bar = 500µm.

Supp. Fig. 9. Migratory potential of MCF-7 cells with MWCO fraction of conditioned medium-derived from adipose-derived mesenchymal stem cells (ADSC-CM) measured by distance migrated using a scratch wound assay. MCF-7 cells were seeded at confluent densities and treated with <3kDa ADSC-CM for 24 hr. (A) Wound healing assay performed on MCF-7 cells at 0hr and 24 hr time-points in the presence and absence of 2µg/mL Mitomycin-C (Scale bar = 500µm). (B) Migratory potential of MCF-7 cells measured following treatment with <3kDa fraction of-ADSC-CM for 24 hr. *$p<0.05$ versus untreated control. Scale bar = 500µm.

Supp. Fig. 10. Western blot images for active β-catenin. MCF-7 and MDA-MB-231 cells were seeded in 6 well plates or 24 well plates and treated with conditioned medium-derived from adipose-derived mesenchymal stem cells (indicated as CM) in the presence and absence of sFRP4 for 72 hr. Effect of treatments on protein expression of active β-catenin in (A) MCF-7, and (B) MDA-MB-231 tumour cell lines.

Supp. Fig. 11. Western blot images for Bcl-xL. MCF-7 and MDA-MB-231 cells were seeded in 6 well plates or 24 well plates and treated with conditioned medium-derived from adipose-derived mesenchymal stem cells (indicated as CM) in the presence and absence of

sFRP4 for 72 hr. Effect of treatments on protein expression of Bcl-xL in (A) MCF-7, and (B) MDA-MB-231 tumour cell lines.

Supp. Fig. 12. Western blot images for Cyclin D1. MCF-7 and MDA-MB-231 cells were seeded in 6 well plates or 24 well plates and treated with conditioned medium-derived from adipose-derived mesenchymal stem cells (indicated as CM) in the presence and absence of sFRP4 for 72 hr. Effect of treatments on protein expression of Cyclin D1 in (A) MCF-7, and (B) MDA-MB-231 tumour cell lines.

Figure 1

Click here to download high resolution image

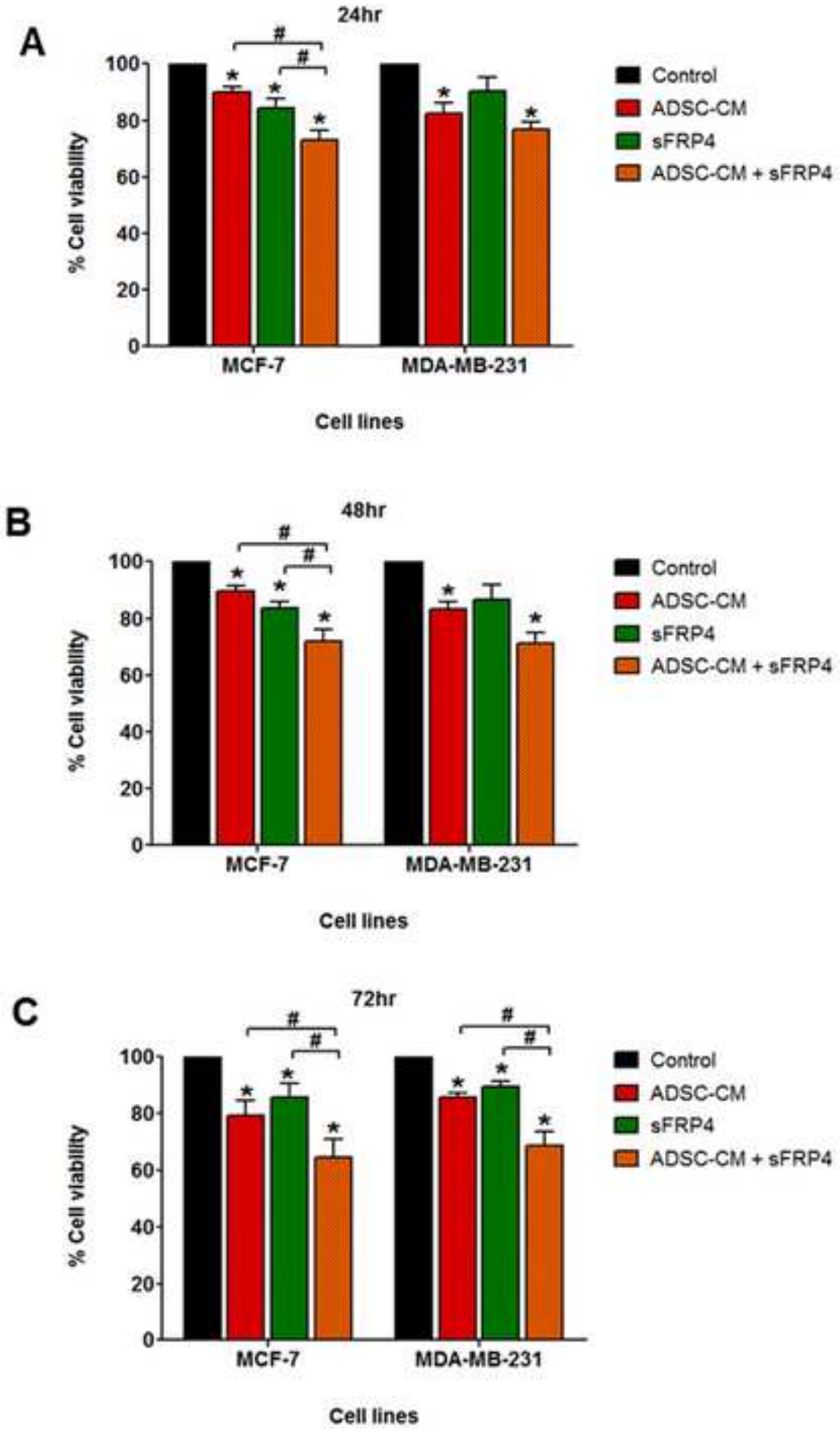

Figure 2

Click here to download high resolution image

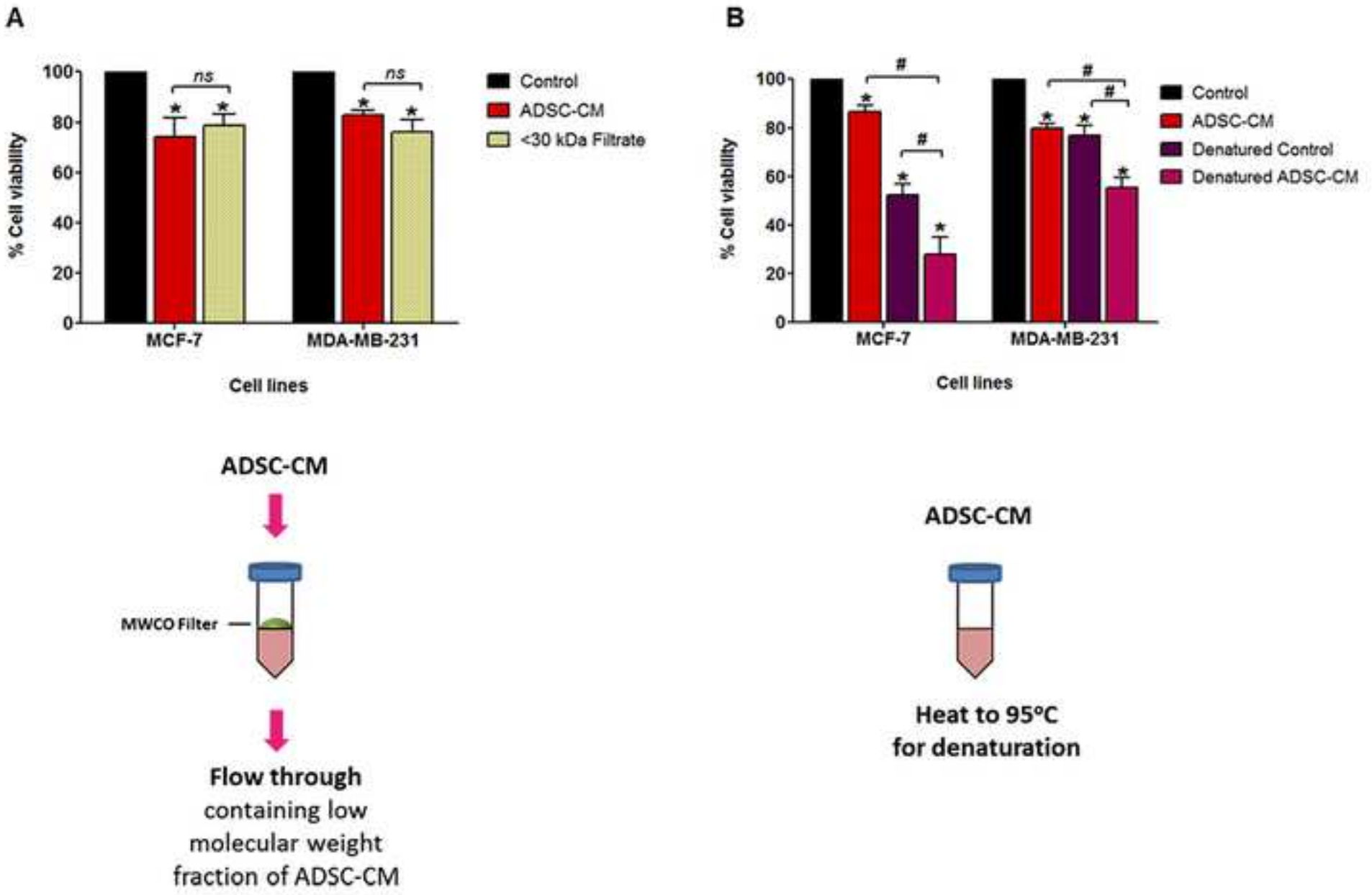

Figure 3

Click here to download high resolution image

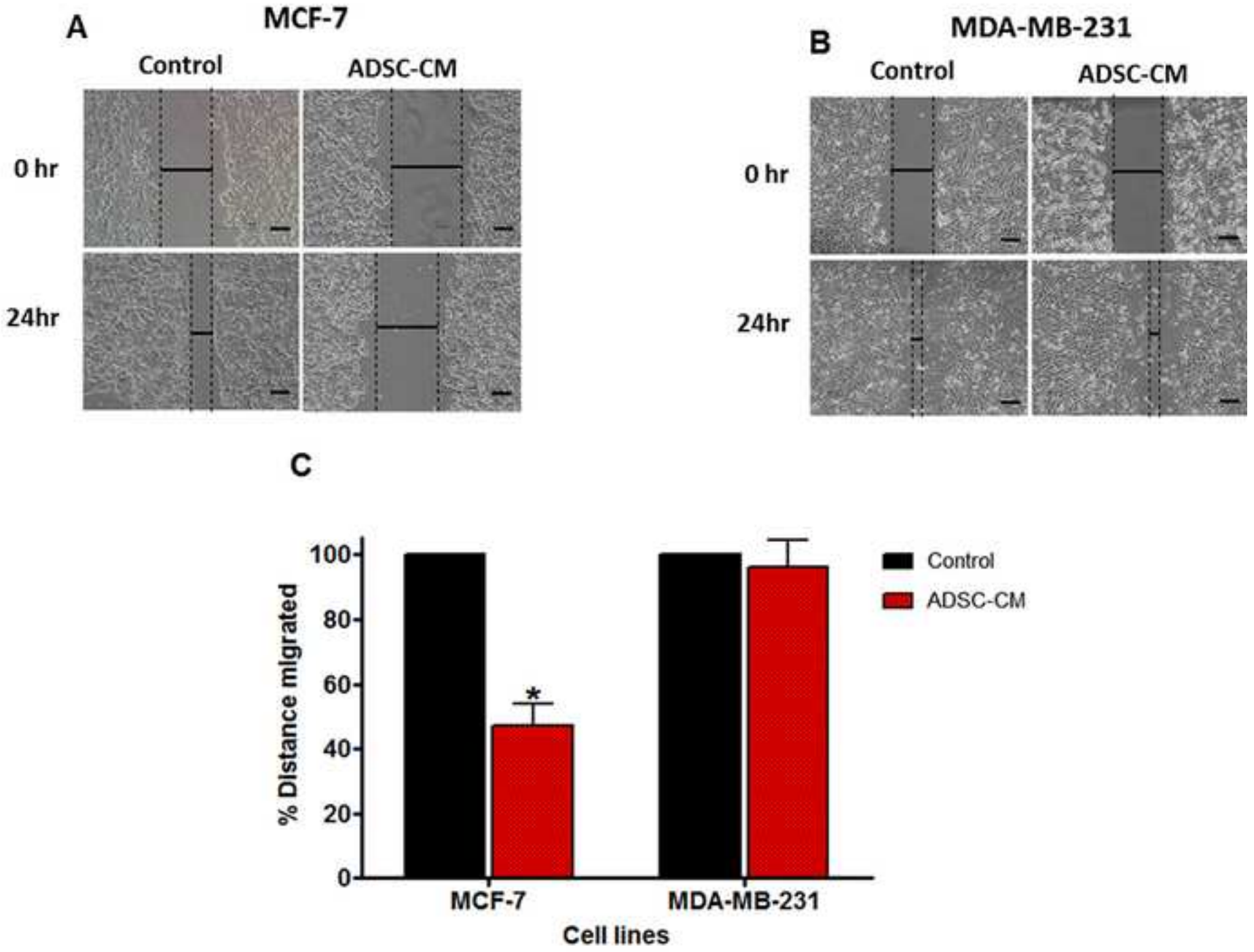

Figure 4
Click here to download high resolution image

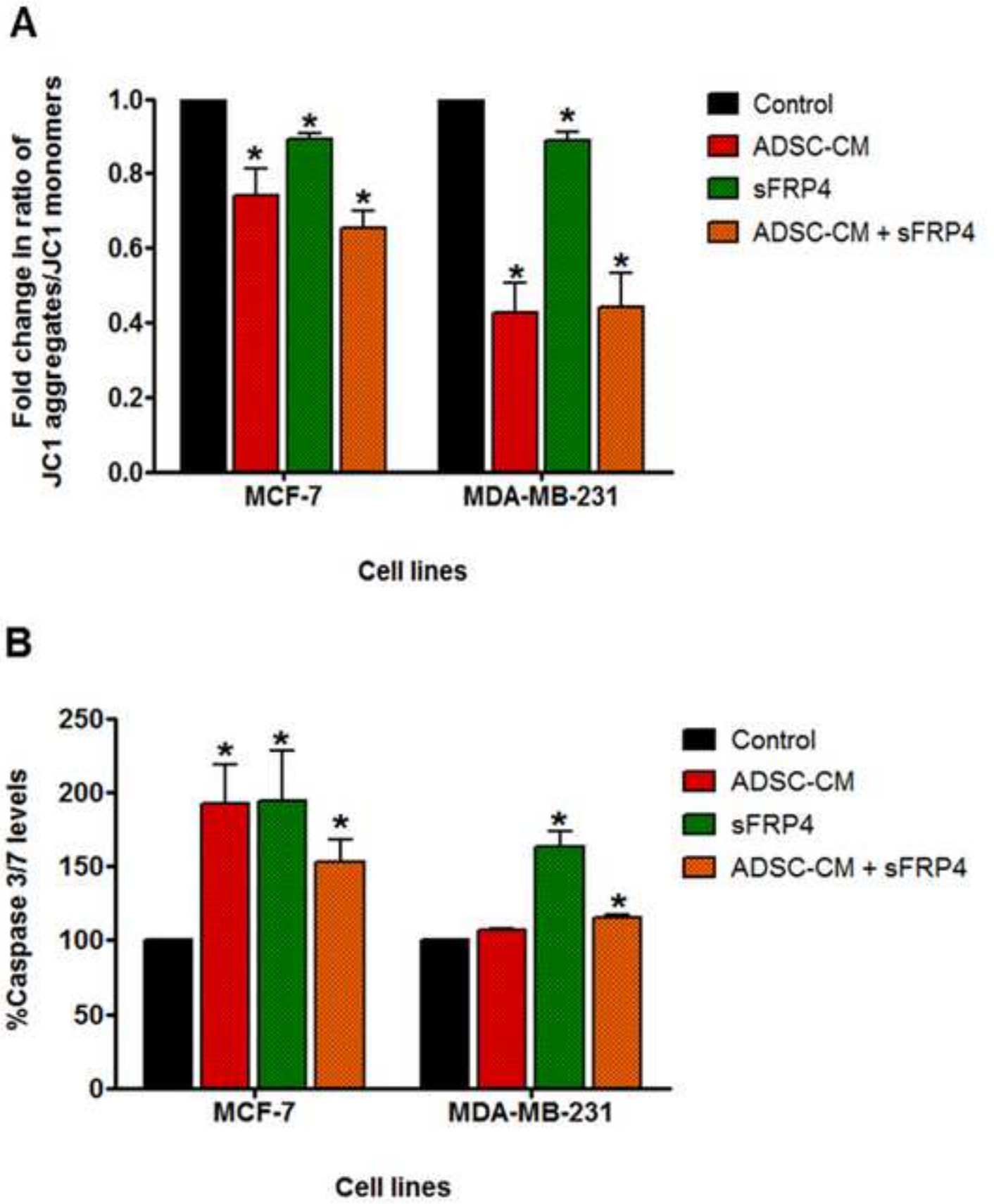

Figure 5

Click here to download high resolution image

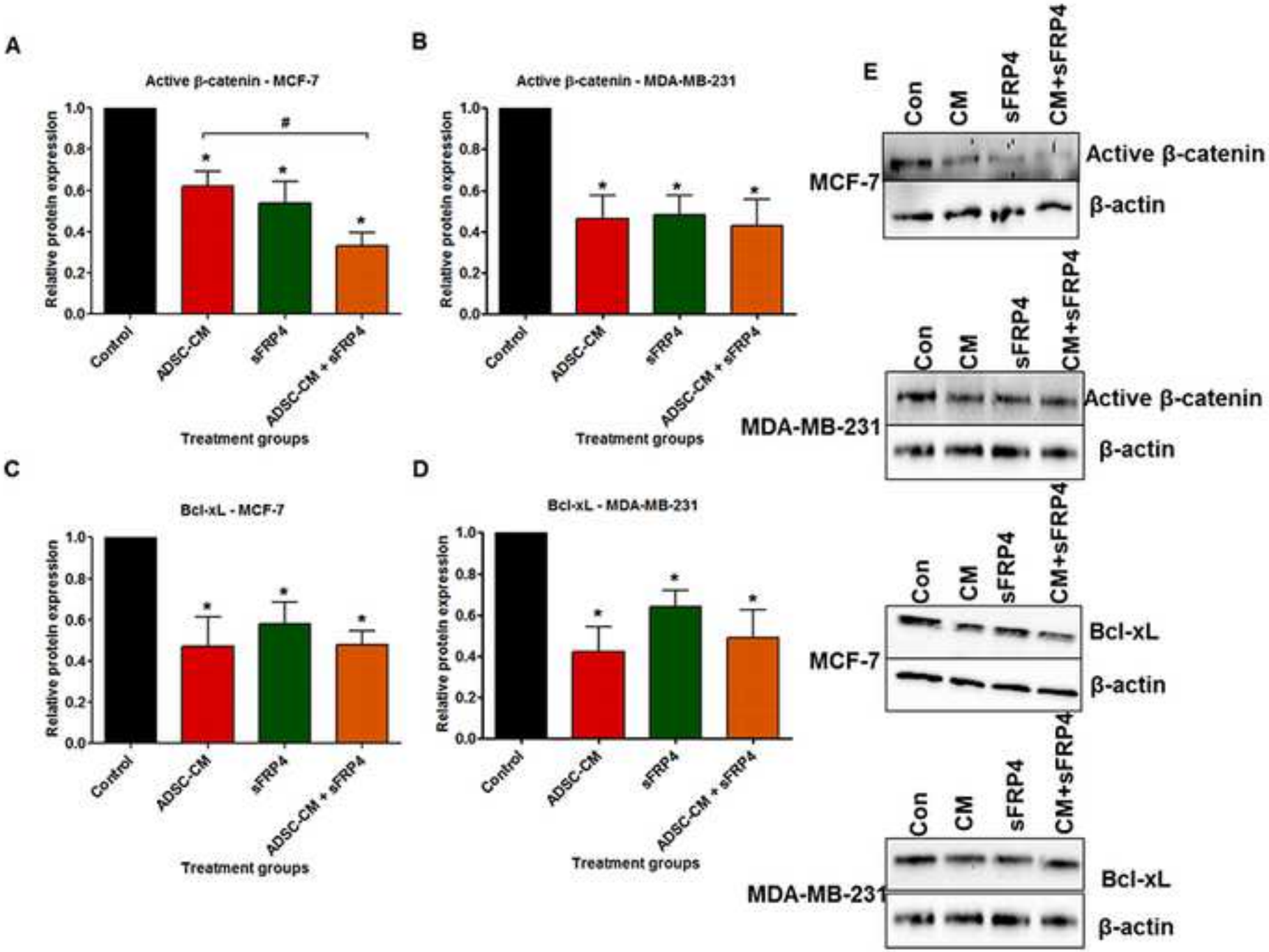

Figure 6

Click here to download high resolution image

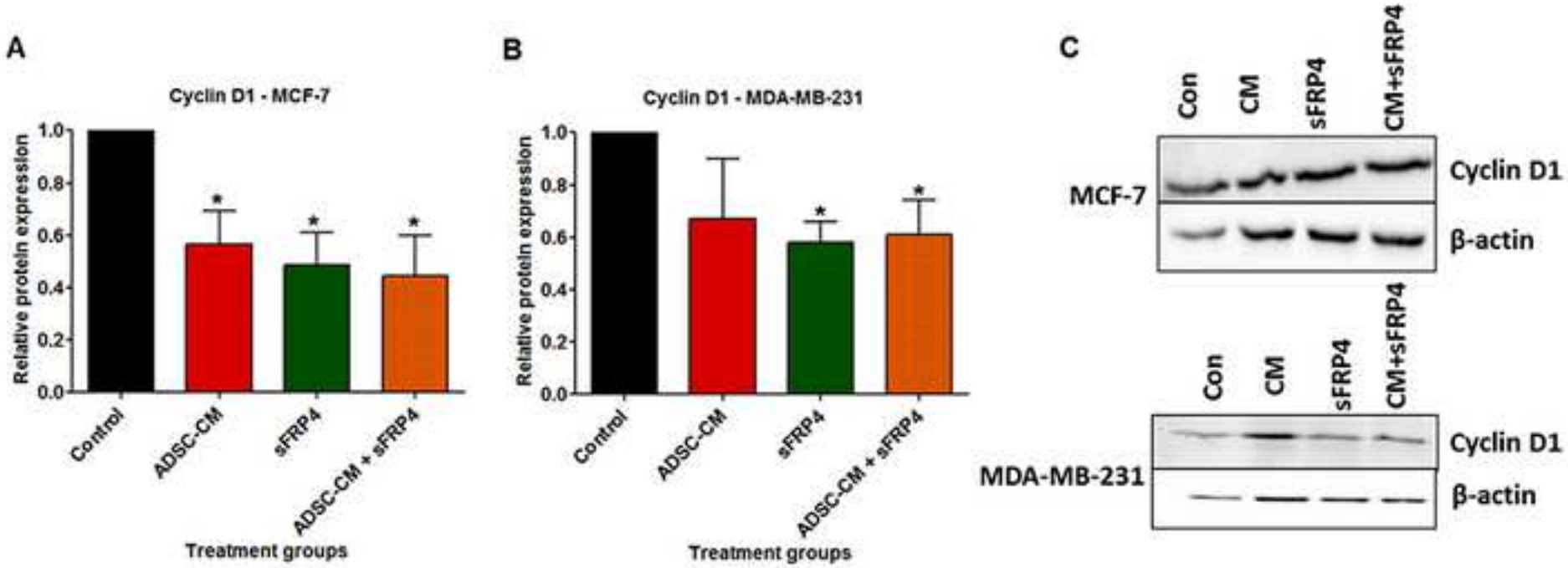

Figure 7
Click here to download high resolution image

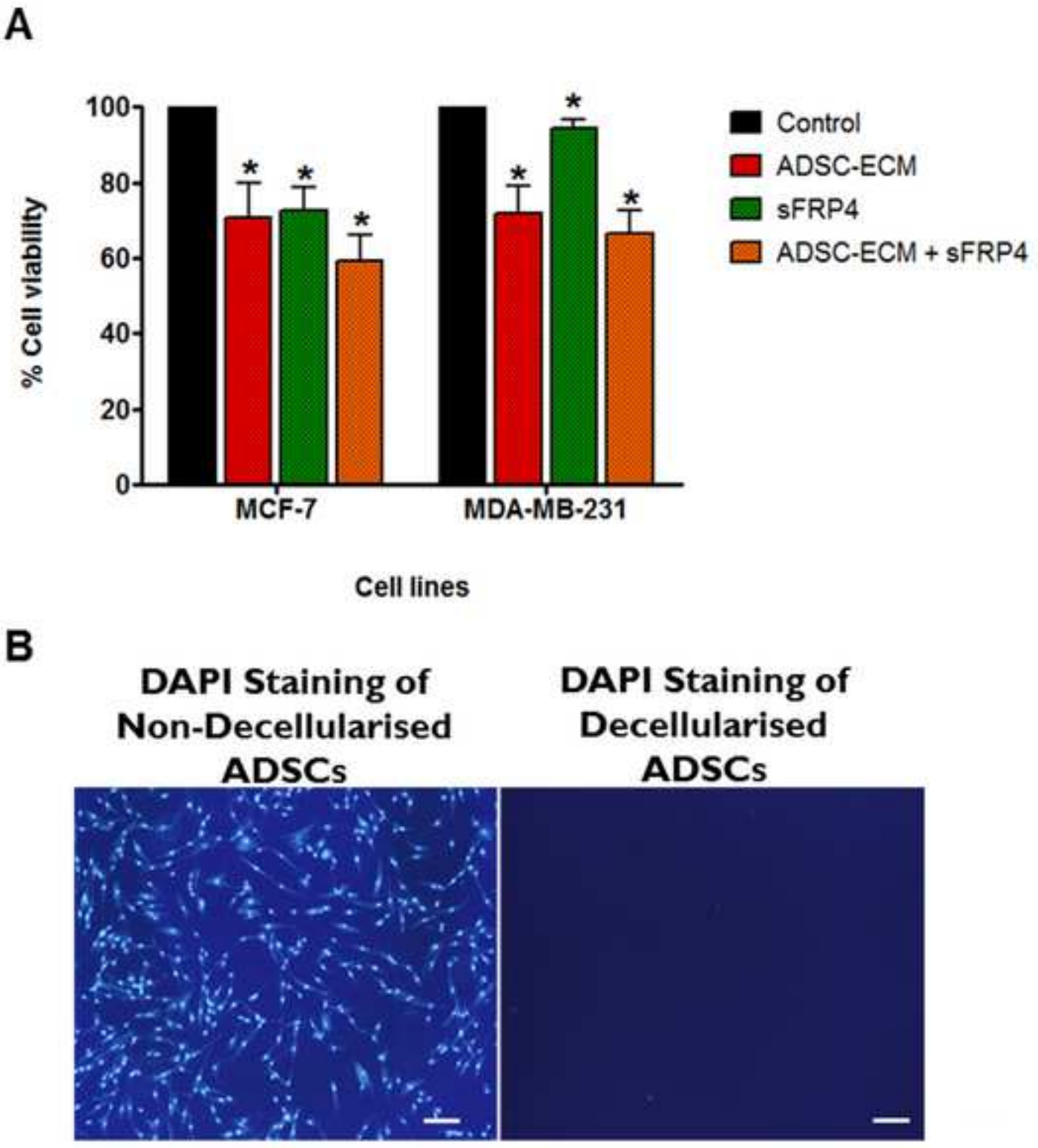

Supplementary File 1

Click here to download Supplementary Files: Supp Fig 1.tif

Supplementary File 2

Click here to download Supplementary Files: Supp Fig 2.tif

Supplementary File 3

Click here to download Supplementary Files: Supp Fig 3.tif

Supplementary File 4

Click here to download Supplementary Files: Supp fig 4.tif

Supplementary File 5

Click here to download Supplementary Files: Supp Fig 5.tif

Supplementary File 6

Click here to download Supplementary Files: Supp Fig 6.tif

Supplementary File 7

Click here to download Supplementary Files: Supp Fig 7.tif

Supplementary File 8

Click here to download Supplementary Files: Supp Fig 8.tif

Supplementary File 9

Click here to download Supplementary Files: Supp Fig 9.tif

Supplementary File 10

Click here to download Supplementary Files: Supp fig 10.tif

Supplementary File 11

Click here to download Supplementary Files: Supp fig 11.tif

Supplementary File 12

Click here to download Supplementary Files: Supp fig 12.tif